An *ab initio* intermolecular potential for the carbon monoxide dimer $(CO)_2$

A. van der Pol, A. van der Avoird, and P. E. S. Wormer
Institute of Theoretical Chemistry, University of Nijmegen, Toernooiveld, 6525 ED Nijmegen, The Netherlands

(Received 13 October 1989; accepted 8 March 1990)

We have constructed an analytical potential energy surface for CO–CO by means of *ab initio* calculations for the electrostatic and first-order exchange interactions and by the use of accurate dispersion coefficients recently calculated in our group. Parameter-free damping functions account for second-order exchange and penetration effects. The anisotropy of this potential is represented by an expansion in spherical harmonics for the molecules A and B, up to $L_A, L_B = 5$ inclusive. The second virial coefficients calculated with this potential, including quantum corrections, lie within the experimental error bars over a wide temperature range.

I. INTRODUCTION

A powerful method for obtaining detailed information on the anisotropic intermolecular potentials between small molecules is given by *ab initio* electronic structure calculations. This is exemplified by an *ab initio* N_2–N_2 potential,[1,2] which has been used to evaluate second virial coefficients,[2,3] various transport properties[4] and liquid state data,[3] as well as many properties of interest in the different (orientationally ordered and disordered) phases of solid nitrogen.[5–10] Carbon monoxide is isoelectronic to N_2; its bulk properties are similar to those of nitrogen in some respects, but one has found several characteristic phenomena which are probably related to the (head–tail) asymmetry in the intermolecular potential of CO (as compared with N_2). In particular, there have been extensive structural, thermodynamic, and spectroscopic studies[11–19] on the head–tail disorder in solid α-CO and on the dynamics of related reorientational processes. Theoretical investigations[20,21] addressing these problems, which have started by the construction of an elaborate semiempirical potential, emphasize the need for an accurate CO–CO potential. In earlier studies[22–24] it was assumed that CO has the same symmetry as N_2. It is of special interest to obtain quantitative information on the breaking of this symmetry, both in the long-range and the short-range contributions to the intermolecular potential.

Here, we present a complete anisotropic potential between (rigid) CO molecules. The anisotropic dispersion coefficients C_6, C_7, C_8, C_9, and C_{10} have been taken from accurate *ab initio* calculations by Rijks and Wormer.[25] The calculation of the electrostatic and exchange contributions to the potential is described in Sec. II. The computational procedure has been designed to give the complete potential in analytical form, with its anisotropy represented explicitly in the form of a spherical expansion. Rather than trying to calculate the complete potential at once, from a supermolecular calculation with its inherent basis set superposition error,[26] we have added the (second-order) dispersion energy to the (first-order) electrostatic and exchange interactions. A damping function similar to the form proposed by Tang and Toennies[27] is used to correct the long-range dispersion energy for second-order exchange and penetration effects. The parameters in this damping function are completely determined by the (*ab initio*) first-order exchange results. In Sec. III we check this *ab initio* potential by computation of the second virial coefficients and comparison with the experimental data[28,29] over a wide temperature range.

II. REPRESENTATION AND CALCULATION OF THE ANISOTROPIC POTENTIAL

The intermolecular potential between two linear molecules can be expanded as follows[26]:

$$V(\mathbf{R},\hat{\mathbf{r}}_A,\hat{\mathbf{r}}_B) = (4\pi)^{3/2} \sum_{L_A L_B L} v_{L_A L_B L}(R) A_{L_A L_B L} \times (\hat{\mathbf{R}},\hat{\mathbf{r}}_A,\hat{\mathbf{r}}_B), \tag{1}$$

with the complete orthonormal set of angular functions given by

$$A_{L_A L_B L}(\hat{\mathbf{R}},\hat{\mathbf{r}}_A,\hat{\mathbf{r}}_B) = \sum_{M_A M_B M} \begin{pmatrix} L_A & L_B & L \\ M_A & M_B & M \end{pmatrix} \times Y_{L_A M_A}(\hat{\mathbf{r}}_A) Y_{L_B M_B}(\hat{\mathbf{r}}_B) Y_{LM}(\hat{\mathbf{R}}). \tag{2}$$

The vector $\mathbf{R} = (R,\hat{\mathbf{R}}) = (R,\Theta,\Phi)$ points from the center of mass of molecule A to that of molecule B, the unit vectors $\hat{\mathbf{r}}_A = (\theta_A,\phi_A)$ and $\hat{\mathbf{r}}_B = (\theta_B,\phi_B)$ describe the orientations of the respective molecular axes. All these vectors are expressed relative to an arbitrary (space fixed) coordinate frame. The functions $Y_{lm}(\hat{\mathbf{r}})$ are spherical harmonics and the symbol in large brackets is a 3-j coefficient. Since the angular basis is constructed such that it is invariant with respect to rotations of the space fixed coordinate frame, one may use in the calculation of the potential a special frame with $\hat{\mathbf{R}} = (0,0)$ and $\hat{\mathbf{r}}_B = (\theta_B,0)$ and vary only the "internal" angles θ_A, θ_B and $\phi = \phi_A - \phi_B$ of the AB dimer. The expansion coefficients can then be written as[1,2,26]

$$v_{L_A L_B L}(R) = \pi^{1/2} \int_0^\pi \sin\theta_A \, d\theta_A \int_0^\pi \sin\theta_B \, d\theta_B \int_0^{2\pi} d\phi \times A_{L_A L_B L}(\theta_A,\theta_B,\phi) V(R,\theta_A,\theta_B,\phi). \tag{3}$$

The equivalence of the monomers in CO–CO leads to the symmetry relation

$$V(R,\theta_A,\theta_B,\phi) = V(R,\pi-\theta_B,\pi-\theta_A,\phi) \tag{4}$$

and hence

$$v_{L_A L_B L}(R) = (-1)^L v_{L_B L_A L}(R). \tag{5}$$

 0021-9606/90/127498-07$03.00

The invariance of Eq. (1) under space inversion allows nonzero expansion coefficients only for even values of $L_A + L_B + L$.

There are three advantages in using this expansion. First, it yields an analytic expression for the potential which shows explicitly its dependence on the molecular orientations with respect to a general coordinate frame. Secondly, this expression, in contrast with site–site models, yields in principle an exact representation of the potential surface. In practice, one can represent the potential to any accuracy by truncating the summation in Eq. (1) at values of L_A, L_B and L which are sufficiently large. Finally, we note that this expansion, being in terms of coupled spherical harmonics, is convenient in scattering calculations and calculations of the second virial coefficient,[30] in calculations of the bound states of van der Waals dimers[31] and in lattice dynamics calculations which include large amplitude motions of the molecules.[5–10]

In correspondence with the different first- and second-order interactions that contribute to the CO–CO potential, we can approximate the expansion coefficients by

$$v_{L_A L_B L}(R) = v^{\text{elec}}_{L_A L_B L}(R) + v^{\text{exch}}_{L_A L_B L}(R) + v^{\text{disp}}_{L_A L_B L}(R). \tag{6}$$

The induction interactions may be neglected since they are very small, at all distances, in comparison with the other interactions. The electrostatic interactions are directly given in the form of a spherical expansion with the following well-known closed expression

$$\begin{aligned} v^{\text{elec}}_{L_A L_B L}(R) = {} & (-1)^{L_A} \delta_{L_A + L_B, L} \\ & \times \left[\frac{(2L_A + 2L_B)!}{(2L_A + 1)!(2L_B + 1)!} \right]^{1/2} \\ & \times Q_{L_A} Q_{L_B} R^{-L-1}, \end{aligned} \tag{7}$$

where the Kronecker delta ensures that only the coefficients with $L_A + L_B = L$ are nonvanishing, and Q_{L_A} and Q_{L_B} are the multipole moments of the (linear) molecules A and B. These multipole moments are calculated for $L_A, L_B = 1$ to 5, from the monomer SCF (self-consistent field) wave functions of CO (see Table I). Since the SCF method gives the wrong sign for the (very small) dipole moment of CO and the values calculated[32] by MBPT (many-body perturbation theory) and by SDCI (singly and doubly excited configuration interaction) are rather different, we have used the experimental dipole moment[33] in the final potential. For the higher multipole moments the differences between the values including correlation corrections[32] and the SCF values are not very significant; so, we have retained the latter. The experimental quadrupole moment[33] lies close to the calculated values (see Table I).

The dispersion contributions to the expansion coefficients are written as follows

$$v^{\text{disp}}_{L_A L_B L}(R) = -\sum_{n=6,7,\ldots} f_n^{L_A L_B L}(R) C_n^{L_A L_B L} R^{-n}. \tag{8}$$

The anisotropic long range dispersion coefficients C_n have been calculated for $n = 6,7,8,9,10$ by the time-dependent coupled Hartree-Fock method and the MBPT method by Rijks and Wormer.[25] Through recoupling of the multipole transition moments involved[34] one can directly obtain the coefficients $C_n^{L_A L_B L}$ that must be substituted into Eq. (8) (see Table II). The damping functions $f_n(R)$, which are determined by the form of the first-order exchange interactions, will be discussed below.

Next, we describe the computation of the expansion coefficients $v^{\text{exch}}_{L_A L_B L}(R)$ for the first-order exchange energy. This quantity is defined by the Heitler–London formula

$$\begin{aligned} V^{(1)} = {} & \frac{\langle \mathscr{A} \psi_0^A \psi_0^B | H | \mathscr{A} \psi_0^A \psi_0^B \rangle}{\langle \mathscr{A} \psi_0^A \psi_0^B | \mathscr{A} \psi_0^A \psi_0^B \rangle} \\ & - \langle \psi_0^A | H^A | \psi_0^A \rangle \\ & - \langle \psi_0^B | H^B | \psi_0^B \rangle, \end{aligned} \tag{9}$$

where H^A and H^B are the Hamiltonians of the monomers A and B, H is the dimer Hamiltonian, ψ_0^A and ψ_0^B are the monomer ground state wave functions and $\mathscr{A}$ is the intermolecular antisymmetrizer. We calculate the Heitler–London energy on a grid of orientations $(\theta_A, \theta_B, \phi)$. This grid is chosen such that it corresponds with Gauss–Legendre quadrature for the angles θ_A and θ_B and Gauss-Chebyshev quadrature for the angle ϕ. Substituting for $V(R, \theta_A, \theta_B, \phi)$ the values of the Heitler–London energy at these quadrature points and using the appropriate weights,[35] we can perform the integrations in Eq. (3) numerically.[1,2] By this procedure we obtain the spherical expansion coefficients $v_{L_A L_B L}(R)$ that represent the complete Heitler–London energy and, thus, the electrostatic as well as first-order exchange interactions. The long range electrostatic (multipole–multipole) interactions are given by Eq. (7), with the multipole moments Q_{L_A} and Q_{L_B} that are obtained from the monomer wave functions ψ_0^A and ψ_0^B. We can easily subtract

TABLE I. Monomer properties of CO. Energies in hartree, multipole moments in $ea_0^{L_A}$.

		SCF (this work)	MBPT(4) (Ref. 32)	SDCI (Ref. 32)	Experiment (Ref. 33)
Total energy		−112.778 074	−113.127 945	−113.085 516	
Dipole	($L_A = 1$)	−0.0979	0.0963	0.0411	0.0432
Quadrupole	($L_A = 2$)	−1.5241	−1.5201	−1.5151	−1.44
Octupole	($L_A = 3$)	4.433		3.876	
Hexadecapole	($L_A = 4$)	−10.239		−9.381	
32-pole	($L_A = 5$)	16.684			

TABLE II. Long range interaction coefficients. Dispersion coefficients which are smaller than 0.1% of the leading coefficient have been omitted.

			Electrostatic	Dispersion (Ref. 25)		
L_A	L_B	L	$C_{L+1}^{L_A L_B L}$ (kJ mol^{-1} nm^{L+1})	$C_6^{L_A L_B L}$ (kJ mol^{-1} nm^6)	$C_8^{L_A L_B L}$ (kJ mol^{-1} nm^8)	$C_{10}^{L_A L_B L}$ (kJ mol^{-1} nm^{10})
0	0	0		5.1382(− 3)	5.4187(− 4)	5.7308(− 5)
1	1	0			1.8858(− 5)	− 5.1742(− 6)
1	1	2	− 5.9280(− 4)		− 4.2671(− 5)	− 1.0453(− 5)
2	0	2		2.8605(− 4)	1.6963(− 4)	2.7475(− 5)
2	2	0		7.3106(− 6)	2.5651(− 6)	1.8231(− 6)
2	2	2		8.7374(− 6)	− 4.5294(− 6)	− 3.0602(− 6)
2	2	4	4.2341(− 3)	7.0334(− 5)	2.1237(− 5)	9.9527(− 6)
3	1	2			− 4.3185(− 7)	7.5722(− 7)
3	1	4	− 2.4087(− 4)		1.6622(− 6)	− 2.0985(− 6)
3	3	6	− 2.6027(− 4)		− 5.6233(− 7)	2.0925(− 7)
4	0	4			− 5.5223(− 6)	2.1679(− 6)
4	2	6	1.5927(− 4)		− 2.0609(− 6)	− 2.0722(− 7)
4	4	8	1.1488(− 5)			1.7620(− 7)
5	1	6	− 3.1093(− 6)			1.2322(− 7)
5	3	8	− 6.4421(− 6)			− 5.1015(− 8)

			Dispersion (Ref. 25)	
			$C_7^{L_A L_B L}$ (kJ mol^{-1} nm^7)	$C_9^{L_A L_B L}$ (kJ mol^{-1} nm^9)
1	0	1	4.2998(− 4)	7.4197(− 5)
2	1	1	7.8675(− 6)	7.8477(− 6)
2	1	3	− 2.5695(− 5)	− 1.9223(− 5)
3	0	3	− 1.1557(− 5)	1.6073(− 5)
3	2	3	− 2.7343(− 7)	− 1.4372(− 7)
3	2	5	− 3.6539(− 6)	6.3944(− 7)
4	1	3		− 1.9272(− 7)
4	1	5	− 3.3208(− 5)	8.6186(− 7)
4	3	7	− 5.1025(− 5)	− 2.8712(− 7)
5	0	5		− 6.6206(− 7)
5	2	7	1.7511(− 5)	− 2.9273(− 7)
5	4	9	1.6377(− 6)	

$$v_{L_A L_B L}^{\text{exch}}(R) = v_{L_A L_B L}^{\text{Heitler-London}}(R) - v_{L_A L_B L}^{\text{elec}}(R) \quad (10)$$

and let the expansion coefficients $v_{L_A L_B L}^{\text{exch}}(R)$ represent both the (dominant) first-order exchange and the (electrostatic) charge cloud penetration effects.

We have established that a grid of 6 angles θ_A and θ_B in the interval $0 \leqslant \theta \leqslant \pi$ and 5 angles ϕ in the interval $0 \leqslant \phi \leqslant \pi$ is sufficient to obtain all the spherical expansion coefficients up to $L_A = 5$ and $L_B = 4$ (and vice versa), see Table III. Using the equivalence of the CO molecules, see Eq. (4), we have calculated the Heitler–London energy at 105 orientations of the molecules, for three distances: $R = 5.5$, 6.5, and 7.5 bohr. The distance dependence of the expansion coefficients $v_{L_A L_B L}^{\text{exch}}(R)$ for the exchange and penetration interactions has been represented by three different forms:

$$v_{L_A L_B L}^{\text{exch}}(R) = v_{L_A L_B L}^{\text{exch}}(R_0) \times \exp[- \alpha^{L_A L_B L}(R - R_0) - \beta^{L_A L_B L}(R - R_0)^2], \quad (11a)$$

$$v_{L_A L_B L}^{\text{exch}}(R) = v_{L_A L_B L}^{\text{exch}}(R_0)\left(\frac{R}{R_0}\right)^{\gamma^{L_A L_B L}} \times \exp[- \delta^{L_A L_B L}(R - R_0)], \quad (11b)$$

and

$$v_{L_A L_B L}^{\text{exch}}(R) = \tilde{v}_{L_A L_B L}^{\text{exch}}(R_0)\exp[- a^{L_A L_B L}(R - R_0)], \quad (11c)$$

where R_0 is an arbitrary fixed distance. In the representations (11a) and (11b) we have taken for $v_{L_A L_B L}^{\text{exch}}(R_0)$ the values of the expansion coefficients calculated at $R_0 = 6.5$ bohr and we have calculated the parameters $\alpha^{L_A L_B L}, \beta^{L_A L_B L}$ or $\gamma^{L_A L_B L}, \delta^{L_A L_B L}$ from the values of the coefficients at $R = 5.5$ and 7.5 bohr. The two parameters $\tilde{v}_{L_A L_B L}^{\text{exch}}(R_0)$ and $a^{L_A L_B L}$ in the representation (11c) have been obtained from a least-squares fit to the values of the corresponding expansion coefficients at $R = 5.5$, 6.5 and 7.5 bohr. Due to the fact that these R points are equidistant and that R_0 is the middle point, it follows that $a^{L_A L_B L} = \alpha^{L_A L_B L}$. The different parameters in the representations (11a) and (11c) are listed in Table III. The parameters in representation (11b) are not given, since this representation yields a potential that is practically identical, for a wide range of distances R and for all orientations, to the representation (11a).

Most terms in the representation (11a) have positive values of $\beta^{L_A L_B L}$, see Table III. For a few terms $\beta^{L_A L_B L}$ is negative, which implies that such terms will eventually blow up for very large R. This is of no practical importance, how-

TABLE III. Short-range interaction parameters. The parameters $v^{\text{exch}}_{L_A L_B L}(R_0)$, $\alpha^{L_A L_B L}$ and $\beta^{L_A L_B L}$, with $R_0 = 6.5$ bohr, occur in the representation of the first-order exchange and penetration energy by Eq. (11a). Equation (11c) contains the parameters $\tilde{v}^{\text{exch}}_{L_A L_B L}(R_0)$ and $a^{L_A L_B L}$. The latter, which are also used in the second order damping functions, Eqs. (8) and (13), are equal to the $\alpha^{L_A L_B L}$ (and therefore not given). Spherical expansion coefficients smaller than 0.5% of the isotropic coefficient have been omitted. For $R > 28$ bohr the coefficients with negative $\beta^{L_A L_B L}$ must be set to zero.

L_A	L_B	L	$v^{\text{exch}}_{L_A L_B L}(R_0)$ (kJ mol^{-1})	$\alpha^{L_A L_B L}$ (nm^{-1})	$\beta^{L_A L_B L}$ (nm^{-2})	$\tilde{v}^{\text{exch}}_{L_A L_B L}(R_0)$ (kJ mol^{-1})
0	0	0	13.944 55	32.295 85	9.511 56	13.699 14
1	0	1	7.550 86	28.546 46	21.004 29	7.260 51
1	1	0	1.396 49	21.074 35	51.059 64	1.269 53
1	1	2	− 2.847 85	23.347 83	38.087 38	− 2.652 40
2	0	2	8.450 99	31.324 72	10.195 23	8.291 67
2	1	1	1.696 06	24.093 04	41.636 14	1.569 22
2	1	3	− 3.633 84	27.101 33	25.879 25	− 3.462 46
2	2	0	1.109 47	27.048 95	25.029 87	1.058 82
2	2	2	− 1.811 63	28.468 85	18.944 42	− 1.748 68
2	2	4	4.963 67	31.456 79	7.777 21	4.892 13
3	0	3	3.013 20	29.224 27	16.001 20	2.924 53
3	1	2	0.405 40	17.507 56	81.370 94	0.348 27
3	1	4	− 1.156 32	24.158 55	35.168 79	− 1.082 84
3	2	1	0.267 80	19.678 11	74.105 19	0.233 20
3	2	3	− 0.512 38	24.429 69	38.176 71	− 0.477 13
3	2	5	1.878 69	29.618 97	12.909 67	1.833 96
3	3	4	0.118 22	16.312 21	103.290 30	0.097 49
3	3	6	− 0.695 57	27.755 23	17.027 04	− 0.673 81
4	0	4	1.544 72	31.079 85	7.658 43	1.522 79
4	1	3	0.186 03	17.209 93	102.454 51	0.153 64
4	1	5	− 0.652 10	26.164 14	31.195 66	− 0.615 21
4	2	2	0.111 50	18.752 43	98.317 26	0.092 81
4	2	4	− 0.269 33	26.986 53	24.718 17	− 0.257 18
4	2	6	1.173 49	32.434 34	1.568 09	1.170 06
4	3	5	0.069 61	19.757 10	87.188 63	0.059 15
4	3	7	− 0.490 71	31.097 66	5.671 44	− 0.485 55
4	4	8	0.379 22	34.961 43	− 8.782 19	0.385 48
5	0	5	0.394 00	30.459 86	7.985 77	0.388 17
5	1	6	− 0.165 61	25.679 89	26.619 33	− 0.157 58
5	2	7	0.365 05	32.797 17	− 2.239 90	0.366 58
5	3	8	− 0.158 80	32.103 22	− 3.610 63	− 0.159 87
5	4	9	0.141 40	36.294 47	− 15.655 32	0.145 59

ever, if we truncate those terms at their minimum values, because these minima occur always for $R > 28$ bohr and the short-range interactions are completely negligible at these distances. Some other terms have a maximum. All these maxima occur for $R < 5$ bohr and it is reassuring that these terms also have maxima in the representation (11b), approximately at the same values of R. In the latter representation the majority of the terms have maxima, however, because most of the parameters $\gamma^{L_A L_B L}$ are positive (and sometimes large). Although these maxima occur mostly at very small values of R, we prefer the representation (11a) over (11b). The representation (11c) is, of course, simpler. For those orientations of the CO molecules where the exchange repulsion is still noticeable at distances substantially larger than $R = 7.5$ bohr, the potential with representation (11c) begins to deviate from the representations (11a) and (11b) at those distances. This applies in particular to the linear geometries of the $(CO)_2$ dimer, see Fig. 1.

From the values of the parameters $v^{\text{exch}}_{L_A L_B L}(R_0)$ and $\tilde{v}^{\text{exch}}_{L_A L_B L}(R_0)$ in Table III it is clear that the spherical expansion is converging. Coefficients smaller than 0.5% of the

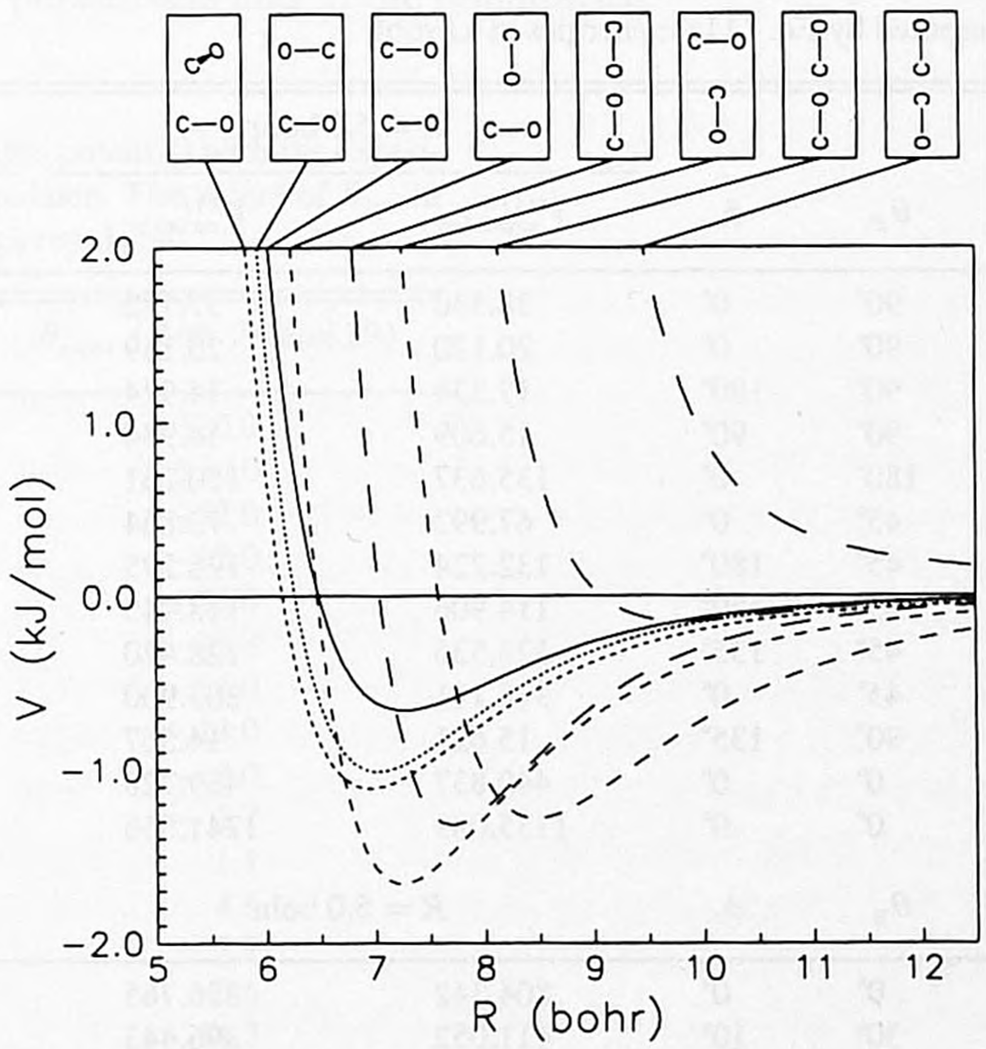

FIG. 1. CO–CO interaction potential for different orientations of the monomers [with the use of the experimental value of the dipole moment and representation (11a) of the exchange repulsion].

isotropic $(L_A,L_B,L) = (0,0,0)$ coefficient have been omitted from Table III. A check of the accuracy of the complete analytic representation of the first-order exchange and electrostatic interactions by comparison with (independent) *ab initio* calculations of the Heitler–London energy at distances and orientations not included in the grid is shown in Table IV.

Let us now return to the damping functions $f_n(R)$ in Eq. (8). For the isotropic interactions between atoms, where the first order overlap repulsion can be fitted to the form $A\exp(-aR)$, Tang and Toennies[27] have proposed to damp the individual terms in the dispersion series

$$V_{\rm disp}(R) = -\sum_n f_n(R) C_n R^{-n} \tag{12}$$

by means of damping functions

$$f_n(R) = 1 - \left[\sum_{k=0}^{n} \frac{(aR)^k}{k!}\right] \exp(-aR), \tag{13}$$

which behave as

$$\begin{aligned} &f_n(R) \to 1 && \text{if } R \to \infty \\ &f_n(R) \to 0 + O(R^{n+1}) && \text{if } R \to 0. \end{aligned} \tag{14}$$

The latter condition can be easily verified by noting that the expression between square brackets in Eq. (13) is the truncated Taylor expansion of $\exp(aR)$.

For the anisotropic interactions between CO molecules we have chosen to damp each (L_A,L_B,L) term in the spherical expansion of the dispersion interactions, Eq. (8), by functions $f_n^{L_A L_B L}(R)$ that have the form of Eq. (13). The parameters $a^{L_A L_B L}$ have been obtained from representation (11c) of the first-order exchange repulsion. As already noted they are equal to the parameters $\alpha^{L_A L_B L}$ appearing in (11a), see Table III. For CO the present damping functions are to be preferred over those used[2] for N_2, which are based on Eq. (11a), because the terms in (11a) that have maxima lead to oscillatory behavior of the damping functions for short distances.

In the actual computations the monomer wave functions ψ_0^A and ψ_0^B are SCF-LCAO functions calculated with the ATMOL package[36] in the Gaussian $(11s,7p,2d/9s,6p,2d)$ basis for C and O, as given in Ref. 37. The CO bond length is fixed at $r = 2.132$ bohr. The orientation vectors $\hat{\mathbf{r}}_A$ and $\hat{\mathbf{r}}_B$ are chosen to point from C to O. The monomer properties calculated in this basis are listed in Table I. Apart from the (very small) dipole moment, which has the wrong sign in any SCF treatment, the ground state of the monomers appears to be well described. This dipole moment is replaced by the experimental value[33] in the final potential, given in Tables II and III; for the overall potential and, in particular, for the second virial coefficients (see below), this makes little difference. In the calculation of the long-range dispersion coefficients by Rijks and Wormer[25] a $(12s,7p,3d,2f/6s,5p,3d,2f)$ basis including more polarization functions has been used. The computation of the Heitler–London energy took about 30 min of CPU time, for each point on the potential surface, on the NAS 9160 university computer at Nijmegen.

This completes the description of the anisotropic CO–CO potential. The terms in this potential with even L_A and L_B are comparable in size with the corresponding terms in the N_2–N_2 potential,[2] both in the long range and the short range. The head–tail asymmetry in CO is reflected by the terms in the spherical expansion with odd L_A and/or L_B. This lack of inversion symmetry is also illustrated by the numerical results in Table IV, by the potential curves in Fig. 1 and by the energy surface in Fig. 2. For the linear geometry of the $(CO)_2$ dimer, for instance, the exchange repulsion is

TABLE IV. Comparison of the spherical expansion of the Heitler–London energy, $V^{(1)} = V^{\rm elec} + V^{\rm exch}$, with direct *ab initio* calculations. Exchange repulsion represented by Eq. (11a); energies in kJ mol^{-1}.

			$R = 5.5$ bohr		$R = 6.5$ bohr		$R = 7.5$ bohr	
θ_A	θ_B	ϕ	$V^{(1)}_{\rm expanded}$	$V^{(1)}_{ab\ initio}$	$V^{(1)}_{\rm expanded}$	$V^{(1)}_{ab\ initio}$	$V^{(1)}_{\rm expanded}$	$V^{(1)}_{ab\ initio}$
0°	90°	0°	38.530	37.782	4.817	4.805	0.252	0.261
90°	90°	0°	20.120	20.159	4.276	4.223	1.187	1.166
90°	90°	180°	17.234	14.974	2.640	2.374	0.403	0.378
90°	90°	90°	15.609	14.954	2.712	2.654	0.517	0.516
0°	180°	0°	135.637	150.261	17.729	19.712	2.852	3.188
45°	45°	0°	67.992	70.864	11.648	12.042	1.420	1.481
45°	45°	180°	132.224	126.295	22.724	21.865	4.000	3.864
135°	45°	180°	114.906	118.445	24.867	25.469	4.632	4.744
135°	45°	135°	123.536	128.420	27.012	27.741	5.057	5.184
135°	45°	0°	316.111	305.900	66.819	65.078	13.992	13.669
90°	90°	135°	15.621	14.567	2.362	2.373	0.345	0.386
0°	0°	0°	440.837	469.728	79.080	82.770	14.140	14.644
180°	0°	0°	1135.089	1241.556	256.586	271.314	55.608	58.243
θ_A	θ_B	ϕ	$R = 5.0$ bohr		$R = 6.0$ bohr		$R = 7.0$ bohr	
30°	0°	0°	804.342	826.765				
30°	30°	10°	411.052	396.443			13.704	13.211
0°	0°	0°			187.831	197.751		
30°	30°	150°					18.434	18.319

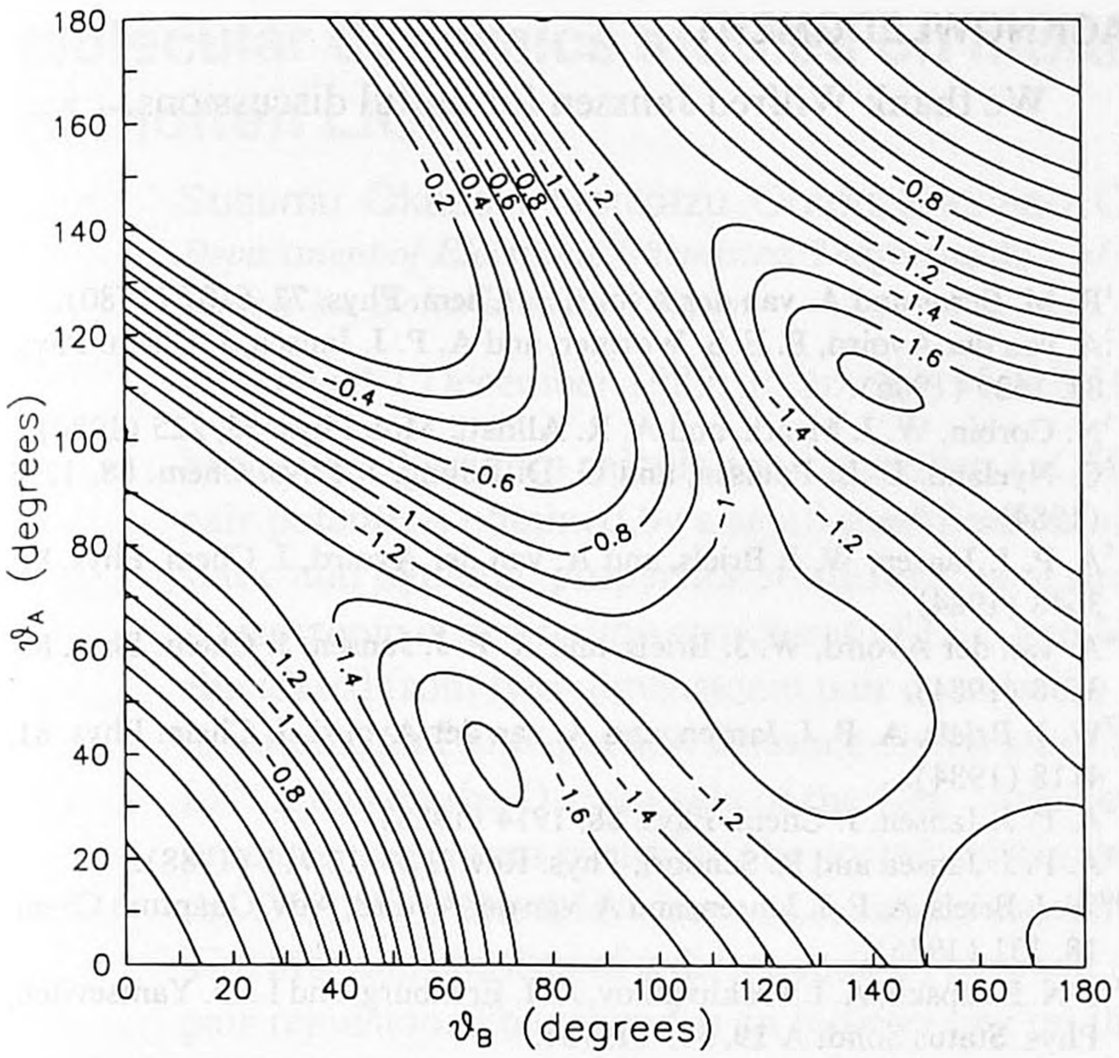

FIG. 2. Orientational dependence of the van der Waals well depth (in kJ/mol) in the CO–CO potential for $\phi = 0°$. Notice the symmetry corresponding with Eq. (4). Orientations without a well (cf. Fig. 1) are found in the upper left-hand corner.

about 10 times larger (at the same distance R) for OC–CO than for CO-OC. This is due to the larger extension of the charge distribution on C, compared with O, and to the fact that the center of mass of CO lies more closely to the O atom. For larger distances this factor increases, which indicates that the charge density decays more steeply around O than around C.

The anisotropy of the CO–CO interaction is displayed as a contour plot in Fig. 2. For most angles ϕ we have found that the T-shaped structure with the O atom of one molecule pointing towards the other molecule ($\theta_A = 0°$, $\theta_B = 85°$, $R_{min} = 7.28$ bohr and $V_{min} = -1.67$ kJ/mol is most stable. For the angle $\phi = 0°$ shown in Fig. 2 there is still a deeper minimum, however ($\theta_A = 40°$, $\theta_B = 70°$, $R_{min} = 7.17$ bohr and $V_{min} = -1.71$ kJ/mol), and for $\phi = 180°$ there is a secondary minimum for a shifted antiparallel structure ($\theta_A = 70°$, $\theta_B = 110°$, $R_{min} = 6.77$ bohr and $V_{min} = -1.66$ kJ/mol. Such small energy differences are within the errors made in the present calculations, however, so the only conclusion we can reasonably draw is that the $(CO)_2$ dimer will show wide-angle oscillations in its vibrational ground state, with low-lying excited states that may have a completely different structure, just as is the case in the $(N_2)_2$ dimer.[38]

III. SECOND VIRIAL COEFFICIENTS

Using the potential presented in the previous section we have calculated the second virial coefficient $B(T)$ over the temperature range (77 K $< T <$ 573 K) in which it has been measured.[28,29] Since our potential has the form of the spherical expansion (1), we can directly use the formulas for two linear molecules presented by Pack.[30] We have included the first quantum corrections due to the relative translational (R) motions, the molecular rotations (A) and the Coriolis term (C):

$$B(T) = B_{clas}(T) + B_R^{(1)}(T) + B_A^{(1)}(T) + B_C^{(1)}(T). \tag{15}$$

The derivatives required in the quantum corrections have been calculated analytically. The integrations over the four-dimensional configuration space have been made by using the same type of quadrature as described in Sec. II for the angles (θ_A, θ_B, ϕ) with $8 \times 8 \times 7$ points and a 100 points trapezoidal rule for the distance R in the range from 4.8 to 45 bohr. In the inner region, $R < 4.8$ bohr, the function $\exp(-V/kT)$ is effectively zero; this yields a constant contribution to the classical term and zero for the quantum corrections. In the outer region, $R > 45$ bohr, all contributions are negligible. We have checked that the results for $B(T)$, given in Table V, are stable against changes in the integration parameters and in the boundaries.

TABLE V. Second virial coefficients (in $cm^3\ mol^{-1}$), calculated from the *ab initio* potential with the experimental dipole moment and representation (11a) of the first-order exchange repulsion. The values of B_{tot} in parentheses are calculated with the simpler representation (11c) of the exchange repulsion.

T(K)	B_{clas}	$B_R^{(1)}$	$B_A^{(1)}$	$B_C^{(1)}$	B_{tot}	B_{exptl} (Refs. 28 and 29)
77.3	−319.74	4.82	6.23	0.31	−308.38 (−299.86)	−320.0
90.1	−234.53	2.91	3.64	0.18	−227.80 (−221.59)	−230.0
143.0	−93.11	0.82	0.92	0.05	−91.34 (−88.55)	−92.0
173.0	−61.05	0.53	0.56	0.03	−59.94 (−57.83)	−62.0
213.0	−35.35	0.34	0.34	0.02	−34.65 (−33.07)	−35.0
242.0	−23.08	0.26	0.26	0.01	−22.54 (−21.20)	−22.8
263.0	−16.21	0.23	0.22	0.01	−15.75 (−14.55)	−16.0
273.0	−13.38	0.21	0.20	0.01	−12.96 (−11.81)	−13.0
298.1	−7.27	0.18	0.17	0.01	−6.91 (−5.88)	−8.0
323.2	−2.28	0.16	0.14	0.01	−1.97 (−1.04)	−3.7
348.2	1.85	0.14	0.12	0.01	2.12 (2.98)	1.1
373.1	5.32	0.12	0.11	0.01	5.55 (6.34)	4.6
398.1	8.28	0.11	0.10	0.01	8.49 (9.23)	7.7
423.2	10.85	0.10	0.09	0.00	11.04 (11.72)	9.6
473.2	15.00	0.08	0.07	0.00	15.15 (15.75)	14.5
513.2	17.63	0.07	0.06	0.00	17.76 (18.31)	17.3
573.2	20.75	0.06	0.05	0.00	20.87 (21.35)	20.5

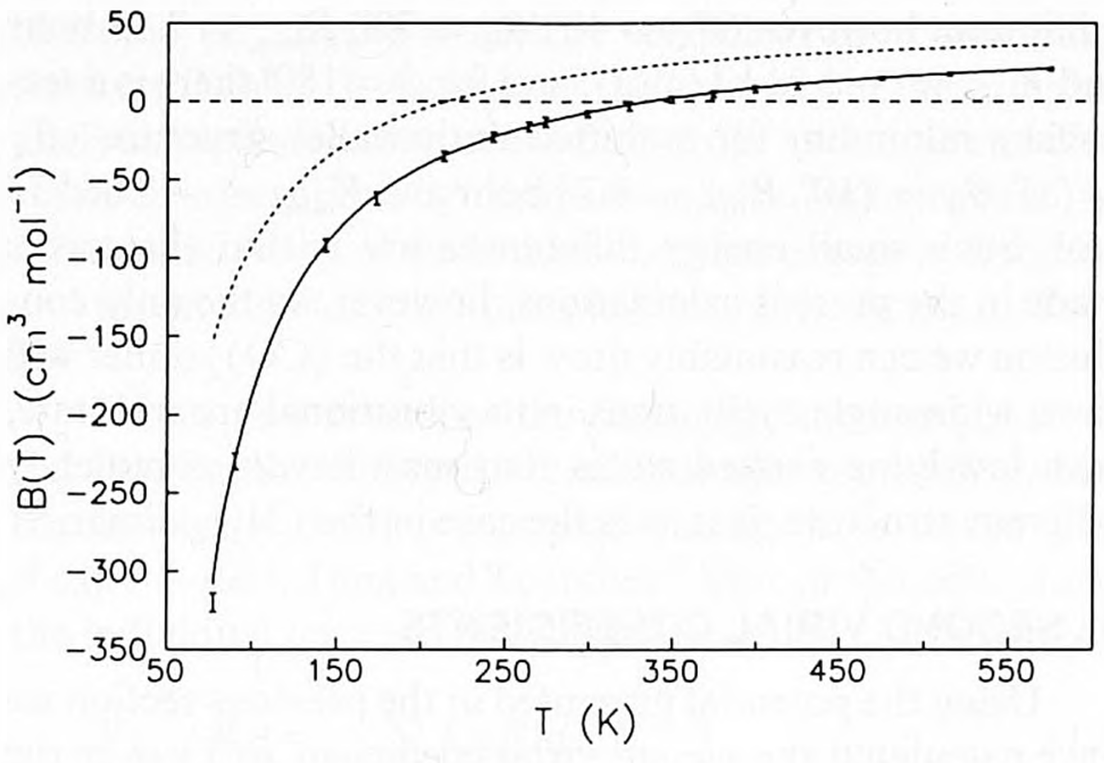

FIG. 3. Second virial coefficients of CO. The experimental data (Refs. 28 and 29) are indicated with (estimated) error bars, the *ab initio* calculations are represented by the closed curve. The dashed curve is the second virial coefficient calculated with the isotropic potential.

The effect of the anisotropy in the potential is quite important (see Fig. 3). The quantum corrections are significant only at the lowest temperatures (see Table V). The Coriolis term is always small. The quantum corrections for the translational motions are practically the same as in nitrogen[2]; the rotational and Coriolis correction terms are more than twice as large. This is caused by the additional anisotropic terms (with odd L_A and/or L_B). The replacement of the calculated dipole moment by the experimental value has little influence on the virial coefficients. The use of the experimental quadrupole moment would not visibly change the curve in Fig. 3. The accuracy indicated for the experimental data[28,29] is typically ± 6 cm^3 mol^{-1} at the lowest temperatures, ± 2 cm^3 mol^{-1} in the middle range and ± 1 cm^3 mol^{-1} at the higher temperatures. We conclude that the *ab initio* CO–CO potential calculated and represented in Sec. II yields a $B(T)$ curve in good agreement with the measured data, practically within the experimental error bars for all temperatures (see Fig. 3). The damping of the dispersion terms in the potential is essential to obtain this agreement. The simpler representation (11c) of the first-order exchange repulsion is somewhat less accurate (see Table V). The virial coefficients calculated with the *ab initio* potential are far better than the data obtained[39] from some empirical anisotropic CO–CO potentials. They are also at least as good as the virial coefficients computed, in a narrower temperature range, from a model potential that has been specifically fitted to the experimental virial coefficients and viscosity data.[40]

Note added in proof: Recently we have been informed by Prof. B. Schramm (private communication) that the latest measurements of the second virial coefficient at 77.3 K yield a value of -307 ± 5 cm^3 mol^{-1}. This brings our calculated value within the experimental error bars, also at this temperature (see Table V and Fig. 3).

ACKNOWLEDGMENT

We thank Wilfred Janssen for useful discussions.

[1]R. M. Berns and A. van der Avoird, J. Chem. Phys. **72**, 6107 (1980).
[2]A. van der Avoird, P. E. S. Wormer, and A. P. J. Jansen, J. Chem. Phys. **84**, 1629 (1986).
[3]N. Corbin, W. J. Meath, and A. R. Allnatt, Mol. Phys. **53**, 225 (1984).
[4]C. Nyeland, L. L. Poulsen, and G. D. Billing, J. Phys. Chem. **88**, 1216 (1984).
[5]A. P. J. Jansen, W. J. Briels, and A. van der Avoird, J. Chem. Phys. **81**, 3648 (1984).
[6]A. van der Avoird, W. J. Briels, and A. P. J. Jansen, J. Chem. Phys. **81**, 3658 (1984).
[7]W. J. Briels, A. P. J. Jansen, and A. van der Avoird, J. Chem. Phys. **81**, 4118 (1984).
[8]A. P. J. Jansen, J. Chem. Phys. **88**, 1914 (1988).
[9]A. P. J. Jansen and R. Schoorl, Phys. Rev. B **38**, 11 711 (1988).
[10]W. J. Briels, A. P. J. Jansen, and A. van der Avoird, Adv. Quantum Chem. **18**, 131 (1986).
[11]I. N. Krupskii, A. I. Prokhvatilov, A. I. Erenburg, and L. D. Yantsevitch, Phys. Status Solidi A **19**, 519 (1973).
[12]H. Suga and S. Seki, Faraday Discuss. **69**, 221 (1980).
[13]K. R. Nary, P. L. Kuhns, and M. S. Conradi, Phys. Rev. B **26**, 3370 (1982).
[14]F. Li, J. Brookeman, A. Rigamonti, and T. A. Scott, J. Chem. Phys. **74**, 3120 (1981).
[15]J. Walton, J. Brookeman, and A. Rigamonti, Phys. Rev. B **28**, 4050 (1983).
[16]S.-B. Liu and M. S. Conradi, Phys. Rev. B **30**, 24 (1984).
[17]A. Anderson and G. E. Leroi, J. Chem. Phys. **45**, 4359 (1966).
[18]A. Ron and O. Schnepp, J. Chem. Phys. **46**, 3991 (1967).
[19]A. Anderson, T. Sun, and M. C. A. Donkersloot, Can. J. Phys. **48**, 2265 (1970).
[20]P. F. Fracassi and M. L. Klein, Chem. Phys. Lett. **108**, 359 (1984).
[21]P. F. Fracassi, R. Righini, R. G. Della Valle, and M. L. Klein, Chem. Phys. **96**, 361 (1985).
[22]T. Shinoda and H. Enokido, J. Phys. Soc. Jpn. **26**, 1353 (1969).
[23]D. A. Goodings and M. Henkelman, Can. J. Phys. **49**, 2898 (1971).
[24]B. Okray-Hall and H. M. James, Phys. Rev. B **13**, 3590 (1976).
[25]W. Rijks and P. E. S. Wormer, J. Chem. Phys. **90**, 6507 (1989).
[26]A. van der Avoird, P. E. S. Wormer, F. Mulder, and R. Berns, Topics Curr. Chem. **93**, 1 (1980).
[27]K. T. Tang and J. P. Toennies, J. Chem. Phys. **80**, 3726 (1984).
[28]J. H. Dymond and E. B. Smith, *The Virial Coefficients of Pure Gases and Mixtures* (Oxford University, Oxford, 1980).
[29]E. Elias, N. Hoang, J. Sommer, and B. Schramm, Ber. Bunsenges. Phys. Chem. **90**, 342 (1986).
[30]R. T. Pack, J. Chem. Phys. **78**, 7217 (1983).
[31]G. Brocks, A. van der Avoird, B. T. Sutcliffe, and J. Tennyson, Mol. Phys. **50**, 1025 (1983).
[32]G. H. F. Diercksen and A. J. Sadlej, Chem. Phys. **96**, 17 (1985).
[33]W. L. Meerts, F. H. de Leeuw, and A. Dymanus, Chem. Phys. **22**, 319 (1977).
[34]P. E. S. Wormer, F. Mulder, and A. van der Avoird, Int. J. Quantum Chem. **11**, 959 (1977).
[35]M. Abramowitz and I. A. Stegun, *Handbook of Mathematical Functions*, Natl. Bur. Stand. (U.S. GPO, Washington, D. C. 1964).
[36]V. R. Saunders and M. F. Guest, SERC Daresbury Laboratory, Wafrington, UK.
[37]R. Schinke, H. Meyer, U. Buck, and G. H. F. Diercksen, J. Chem. Phys. **80**, 5519 (1984).
[38]G. Brocks and A. van der Avoird, Mol. Phys. **55**, 11 (1985).
[39]M. D. Whitmore and D. A. Goodings, Can. J. Phys. **58**, 820 (1980).
[40]S. Singh and Y. Singh, Physica **83** A, 339 (1976).